HEFAT2014
10th International Conference on Heat Transfer, Fluid Mechanics and Thermodynamics
14 – 16 July 2014
Orlando, Florida

A STUDY ON EVALUATION OF EFFECTIVE THERMAL CONDUCTIVITY FOR SPHERICAL CAPSULES

Mehmet Akif Ezan*, Mehmet Uzun, Aytunc Erek
*Author for correspondence
Department of Mechanical Engineering,
Dokuz Eylül University,
Izmir, Turkey,
E-mail: mehmet.ezan@deu.edu.tr

ABSTRACT

The main goal of the current work is to evaluate specific equations to define effective thermal conductivity for inward melting problems inside spherical containers in terms of the temperature difference and the spacing between the interface and shell. Sets of numerical analyses have been conducted with commercial CFD software ANSYS-FLUENT. In order to check the validity of the method, proposed effective thermal conductivity equation has been implemented into a phase change problem inside a spherical container, and the results are compared with the experimental findings. Comparative results reveal that implementation of the effective thermal conductivity yields reasonable results regarding to the experimental measurements

INTRODUCTION

In the design period of thermal energy storage systems, there are several parameters should be taken into account, such as thermo-physical properties of the phase change material, dimensions of the enclosure and working parameters of the secondary-fluid. Since the experimental investigation and optimization of such a system is costly and time consuming, engineers and researchers mainly use numerical simulations to find optimum parameters for a specific application. The main difficulty that may arise while solving a phase change problem is capturing the interface position properly. To do so, there are mainly two solution strategies; moving grid and fixed grid [1]. In the former one, according to the interface position mesh is regenerated at each time step to capture high gradients around the phase change front perfectly. On the other hand, in the latter one, the mesh structure is kept constant for the whole solution period, and the interface position is revealed according to the enthalpy or temperature distribution. Each method has some cons and pros and the details about these methods are of the focus of our current study. Detailed information about these methods can be found elsewhere [2, 3].

The main difficulty, however, may arise for solving a phase change problems if the effects of natural convection cannot be omitted. Such cases correspond almost for all real applications, since the temperature difference between the phase change temperature of the PCM and the secondary fluid may reach10°C to 20°C. The presence of natural convection affects both total time of phase change and the curvature of the interface. Natural convection and thermal stratification phenomena inside an enclosure deteriorate uniformity of phase change front. There are countless studies which deal with the numerical and experimental investigation of natural convection driven phase change. Here we will mainly focus on revealing the time consumed for such analyses.

NOMENCLATURE

C	[-]	Dimensionless heat capacity
g	[m/s^2]	Gravitational acceleration
Gr	[-]	Grashof number
h	[kJ/kg]	Enthalpy
k	[W/mK]	Thermal conductivity
K	[-]	Dimensionless thermal conductivity
L	[m]	Gap of annulus
Nu	[-]	Nusselt number
q	[W]	Rate of heat transfer
p	[Pa]	Pressure
r	[m]	Radial axis direction
R	[-]	Dimensionless radial axis
S	[-]	Dimensionless source term
S'	[-]	Shape factor
Ste	[-]	Stefan number
T	[°C]	Temperature
t	[s]	Time
u	[m/s]	Velocity

Special characters

ε	[-]	Convergence criteria
$\delta\theta_m$	[-]	Dimensionless temperature range of mushy zone
ΔT	[K,°C,°F]	Temperature differences
ρ	[kg/m^3]	Density
θ	[-]	Dimensionless temperature
ϕ	[°]	Angular position
μ		
τ	[-]	Dimensionless time

Subscripts

eff	Effective
i	Inner
m	Melting or Mushy region
o	Outer
s	Solid phase

Tan et al. [4] carried out experimental and numerical study in order to investigate melting period of n-octadecane inside a spherical enclosure. They used commercial CFD software in their simulations and the optimum time step size is obtained to be 0.1 s. Assis et al. [5] considered melting period paraffin inside spherical container. Since they have examined advanced unconstrained melting problem with considering air at the top of the sphere, optimum time-step size became so small such as 0.02 s. Shmueli et al. [6] experimentally and numerically investigated the melting process of paraffin inside vertical cylindrical cavity. The container consists of PCM and air regions so the VOF (Volume of fluid) multiphase model is solved with enthalpy-porosity method. Optimum time-step size of this analysis is represented to be 0.002s. Shatikian et al. [7] presented their numerical findings of inward melting process of a PCM between to fins. Again the authors optimized the time-step size as 0.01s to achieve considerable convergence criteria.

These comprehensive works deal with in-depth analyses of the natural convection driven phase change and aim to reveal local natural convection patterns, thermal stratification regions and variation of the interface as a function of time or space. In such an analysis, in order to decrease the numerical errors for all governing equations, the time-step size has to be kept around 0.1 s or below. Nevertheless, it will be time consuming process to follow such an analysis to carry out engineering design, which requires testing of lots of parameters for a particular problem.

There are also some other methods to simplify natural convection driven phase change problems within a reasonable engineering accuracy. Ismail et al. [8] simulated the inward solidification process inside a sphere with the presence of natural convection. Instead of modelling the natural convection for the liquid phase of the PCM, they have defined effective thermal conductivity to consider the influence of convection. Reasonable consistency has been obtained according to the comparative results of time-wise variation of the temperature at the center of the sphere. However, Ismail et al. [8] indicated that there is no certain correlation to compute the effective thermal conductivity value for spherical containers and the literature values vary between 1.4 W/mK and 8.2 W/mK.

The main goal of this study is to correlate the variation effective thermal conductivity of water as a function of the interface position for inward melting process inside a spherical container.

DEFINITION OF THE PROBLEM

In this study, we have carried out three different sets of numerical analyses. In the first step, in order to obtain the effective thermal conductivity values, steady-state natural convection of water is simulated for various geometric and thermal conditions. The validity of the steady-state analyses has been tested regarding to the experimental data of Bishop et al. [9] for the case of air. As a last step, the correlated data is implemented into a numerical code to simulate inward melting inside a spherical container, and the results are compared against the experimental measurements. Following sub-sections will define each problem and the related solution methods.

Steady-state natural convection of water/air inside sphere

As a first step, steady-state natural convection inside a spherical annulus is considered. As shown in the Figure 1, sphere is considered to be two dimensional and axis-symmetric. The inner and outer radius of the spherical annulus are indicated as r_i and r_o, respectively, and the outer and inner surfaces are kept at constant temperatures as T_o and T_i, respectively. For the each case of fluid, water or air, except the density, thermo-physical properties of the fluid are defined to be constants and are obtained at a mean temperature, $T_{mean} = (T_o + T_i)/2$. Density of water and air are identified as a function of temperature, which is valid for the temperature range considered in this study as

$\rho_{water} = -0.007085T^2 + 3.925T + 456.49$ (kg/m^3)
$\rho_{air} = 1E\text{-}05T^2 - 0.0104T + 3.3209$ (kg/m^3)

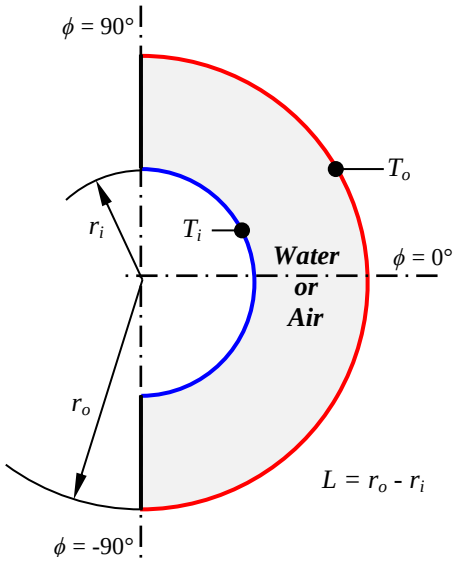

Figure 1 Definition of the problem

Considering the incompressible, two-dimensional, steady-state and laminar flow inside a spherical annulus, governing equations can be reduced as

Continuity

$$\frac{\partial u}{\partial x_i} = 0 \qquad (1)$$

Momentum

$$\frac{\partial}{\partial x_j}\left(\rho u_i u_j\right) = \mu \frac{\partial^2 u_i}{\partial x_j \partial x_j} - \frac{\partial p}{\partial x_i} + \rho g_i \qquad (2)$$

Energy

$$\frac{\partial}{\partial x_i}\left(\rho u_i h\right) = \frac{\partial}{\partial x_i}\left(k \frac{\partial T}{\partial x_i}\right) \qquad (3)$$

For the inner and outer walls of the sphere, no-slip boundary condition is applied. Remaining boundaries (*vertical axis-lines*) are defined to be axis. Governing equations are discretized into algebraic sets of equations with using Control-Volume-Approach of Patankar [10]. Power-Law scheme [10] is

implemented for evaluating the values at the control surfaces for each transport parameter. SIMPLE algorithm is used as a solution algorithm of governing equations. The computational domain is divided into 150.000 structured computational volumes, and the grid density is increased near the outer and inner surfaces of the sphere to capture the higher temperature and velocity gradients. Convergence criteria for the mass, momentum, and energy balance equations are set to be 10^{-6}. Computations are performed with the aid out commercial CFD software ANSYS-FLUENT v.14 [11].

Numerical Investigation of Inward Melting of Water

Melting process of water inside the sphere is investigated both experimentally and numerically. Numerical analyses have been performed with implementing the temperature transforming method of Cao and Faghri [12]. Since the effective conductivity meets the effect of convection, one-dimensional heat conduction with phase change is considered in formulation,

$$\frac{\partial}{\partial \tau}\left(C\theta\right)+\frac{\partial}{\partial \tau}\left(S\right)=\frac{1}{R^2}\frac{\partial}{\partial R}\left(KR^2\frac{\partial \theta}{\partial R}\right) \tag{4}$$

According to this method, enthalpy can be identified as a piece-wise linear functions for liquid, mushy and solid phases in terms of the temperature. *C*, *K* and *S* are defined for each phase of the material as follows,

$$C\left(\theta\right)=\begin{cases} C_S & \theta<-\delta\theta_m \\ 0.5\left(1+C_S\right)+\dfrac{1}{2\mathrm{Ste}\,\delta\theta_m} & -\delta\theta_m\le\theta\le+\delta\theta_m \\ 1 & +\delta\theta_m<\theta \end{cases} \tag{5}$$

$$K\left(\theta\right)=\begin{cases} K_S & \theta<-\delta\theta_m \\ K_S+\left(1-K_S\right)\dfrac{\theta+\delta\theta_m}{2\delta\theta_m} & -\delta\theta_m\le\theta\le+\delta\theta_m \\ 1 & +\delta\theta_m<\theta \end{cases} \tag{6}$$

$$S\left(\theta\right)=\begin{cases} C_S\delta\theta_m & \theta<-\delta\theta_m \\ 0.5\left(1-C_S\right)\delta\theta_m+0.5/\mathrm{Ste} & -\delta\theta_m\le\theta\le+\delta\theta_m \\ C_S\delta\theta_m+1/\mathrm{Ste} & +\delta\theta_m<\theta \end{cases} \tag{7}$$

Here, except the thermal conductivity of water in the liquid phase, the thermo-physical properties of water are defined to be constants for each phase. The thermal conductivity of the liquid water is defined as a function of annulus spacing and the temperature difference between the interface and the shell. Non-dimensional parameters that are used in Equations (4-7) can be found elsewhere [12].

Energy equation (Eq. 4) is discretized by finite volume approach of Patankar [10]. Computational domain is divided into five hundred control volumes. In order to interpolate the variation of the thermal conductivity at the solid/liquid interface, harmonic mean thermal conductivity definition of Patankar [10] has been implemented. Tri-Diagonal Matrix Algorithm (TDMA) has been used to resolve the linear sets of equations. The computer code is developed in MATLAB programming language. As a result of the preliminary analyses, time step size is selected to be, t = 10 s. Convergence criteria, ε, for each time-step is defined in terms of the maximum relative change of temperature between two iterations for the whole domain, and for each time step $\varepsilon < 10^{-14}$ is satisfied.

Experimental Investigation of Inward Melting of Water

In the evaluation of the effective thermal conductivity, the problem is reduced into two-dimensional, steady-state problem without phase change. Hence, the convenience of these simplifications is revealed regarding to the experimental comparisons. In the experiments, a spherical container is used with an inner diameter and wall thickness of 55 mm and 2 mm, respectively. Three thermocouples are used to monitor time-wise variation of temperature; one is at the center of the sphere, and two are at the outer surface of the sphere. In order to obtain a homogenous initial temperature inside the sphere, the water filled container is submerged into brine (40% Ethylene-glycol/Water mixture) which is kept at -28°C and remained in there until the center temperature becomes steady-state. Then the sphere is put into another constant-temperature-bath, which has hot-brine with a predefined temperature for melting experiments. Experiments are carried on since the temperature at the center of the sphere reaches to brine temperature.

RESULTS AND DISCUSSION

Validation of the Method

Numerical methodology is introduced with reproducing the experimental study of Bishop et al. [9]. Bishop and his colleagues took into account natural convection of air inside a spherical annulus with isothermal surfaces. In the experimental study, Bishop varied the spacing ratio (L/r_i) to be 0.19, 0.67, 1.00, 1.50 and 2.14. The temperature difference (T_o - T_i), on the other hand, was changed between 15°F to 100°F. Comparative results are obtained in terms of the average Nusselt number and the flow patterns. Bishop et al. [9] suggested the following correlation for natural convection of air inside annulus,

$$\mathrm{Nu}=0.332\mathrm{Gr}^{0.270}\left(L/r_i\right)^{0.517} \tag{8}$$

On the other hand, in the numerical analyses, the average Nusselt number is calculated as

$$Nu=\frac{qL}{4\pi k\left(\Delta T\right)r_i^2} \tag{9}$$

where q is the heat transfer from inner or outer surface of the sphere.

Comparative results are represented in Table 1 for various spacing ratios and temperature differences. Increasing spacing factor or temperature tends to increase the surface Nusselt number. It is also clear that for higher spacing ratios or temperature differences, the difference between the predicted and the experimental data increases. In the experiments, there may be three-dimensional flow patterns or turbulence effects may occur especially for higher Gr numbers, which are not considered in the current mathematical model. Nevertheless, the predicted results have reasonable consistency with the results of reference work, and the maximum deviation is found to be less than 9%.

Table 1 Comparison of Nusselt Number

Spacing Ratio	ΔT	Nusselt		Difference
		Eq. (11)	*Numerical Results*	
(L/r_i)	(°F)	(-)	(-)	(%)
0.67	25	7.06	6.99	1.0
	61	8.64	8.38	3.1
	100	9.50	9.11	4.1
1.00	25	10.43	10.11	3.1
	61	12.77	12.05	5.6
	100	14.03	13.10	6.7
1.50	25	14.91	14.21	4.7
	61	18.26	16.95	7.2
	100	20.06	18.43	8.1
2.14	25	19.90	18.90	5.0
	61	24.37	22.50	7.8
	100	26.77	24.42	8.8

Bishop indicated that three distinct flow patterns were observed namely, *kidney-shaped-eddy*, *crescent-eddy*, and *falling-vortices*. In Figure 2, these three flow patterns are compared against the flow visualizations of the reference work. In Figure 2(a), flow patterns are represented for $L/r_i = 2.14$. A distortion is observed close to $\phi = 0°$ line for the experimental observations and the shape of the flow pattern looks like a *kidney*. However, the predicted flow pattern does not resemble with the experimental one especially for $-45° < \phi < 45°$. As can be seen in Table 1, this discrepancy induces a deviation of 5% in terms of the surface Nusselt number. On the other hand, as seen in Figure 2(b), for $L/r_i = 0.72$, the domain is dominated by a big circulation cell and the shape is similar to the *crescent*. The center of the circulation cell is observed for $0° < \phi < 45°$ as in the reference work. In Figure 2(c) patterns are given for $L/r_i = 0.19$. Since the spacing is so small for this configuration, at the top of the annulus, $40° < \phi < 90°$, small vortices are observed, and this type of flow patterns is called as *falling vortices*. On the other hand, crescent type flow pattern is dominated for the rest of the domain for $-90° < \phi < 40°$. Comparative results reveal that the numerical method that is used in the current work has a reasonable consistency with experimental findings.

Evaluation of the Effective Thermal Conductivity

During the inward melting process, the interface will move from the outer surface through the center of the sphere. Here, we have calculated the effective thermal conductivity for four spacing factors and five temperature differences to evaluate a correlation that can be used in simplified numerical codes for inward melting. The thermal and geometric parameters that are used to evaluate effective thermal conductivity are listed in Table 2. In the analyses, the temperature of the inner sphere is kept constant at the phase change temperature of water, at 0°C.

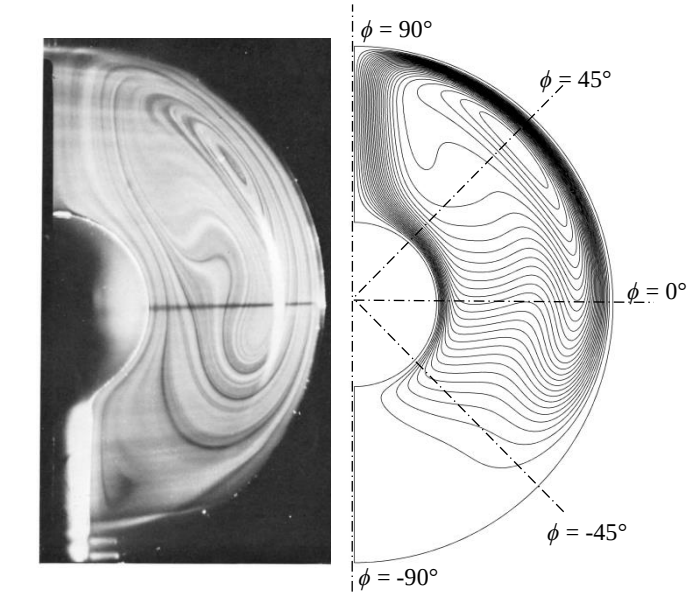

(a) $L/r_i = 2.14$, $\Delta T = 25$°F

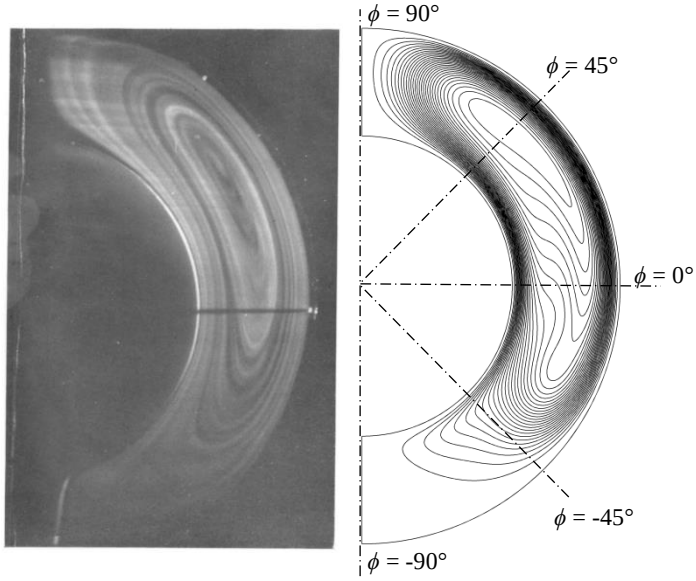

(b) $L/r_i = 0.72$, $\Delta T = 15$°F

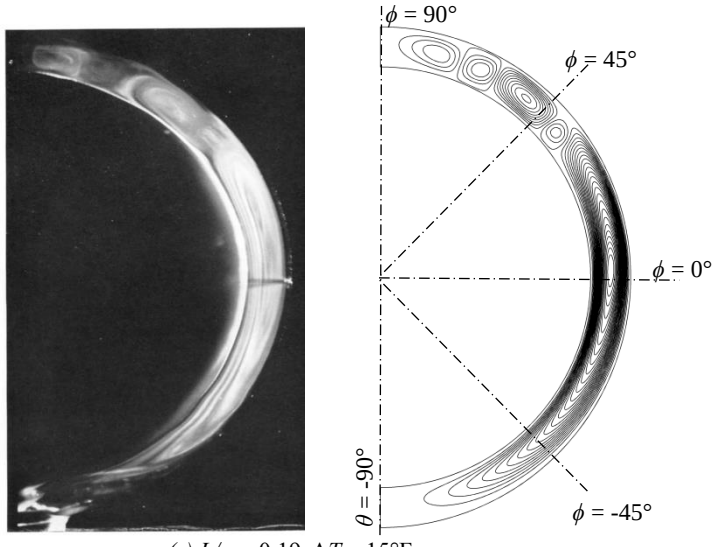

(c) $L/r_i = 0.19$, $\Delta T = 15$°F

Figure 2 Airflow patterns

Table 2 Parameters for steady-state natural convection of water

L/r_i	0.67, 1.00, 1.50 and 2.14
$T_i - T_o$ (°C)	2, 4, 8, 12 and 24

In thermal energy storage systems for cooling applications, owing to the high storage capacity per volume, water is the most popular and appropriate phase change material. However, density inversion of water at 4°C makes it complicate in the mathematical simulations and engineering designs. Regardless from the spacing ratio of the annulus, two discrete flow circulation zones will occur for the cases of surface temperatures higher than 4°C and this will increase the influence of the convective heat transfer on the melting period of the ice. The effective thermal conductivity of a fluid can be defined as

$$q = S' k_{eff} \Delta T \tag{10}$$

where q is evaluated from the numerical analysis and S' is the shape factor of the geometry. For the spherical enclosure, the shape factor becomes,

$$S' = \frac{4\pi}{(1/r_i) - (1/r_o)} \tag{11}$$

In Figure 3, variation of the effective thermal conductivity is given in terms of temperature difference and the spacing ratio. It is clear that increasing the temperature difference and spacing ratio improve the impact of convective forces and enhances the k_{eff}. It is also interesting that, for T_o = 2°C and 4°C, the effective thermal conductivity values are almost identical for all spacing ratios. For the advancing temperature values, on the other hand, the effect of spacing ratio for a particular temperature value becomes clearer. For each outer surface temperature value, k_{eff} is obtained as a function of spacing ratio as 3rd order polynomial functions and the coefficients of these functions are given in Table 3.

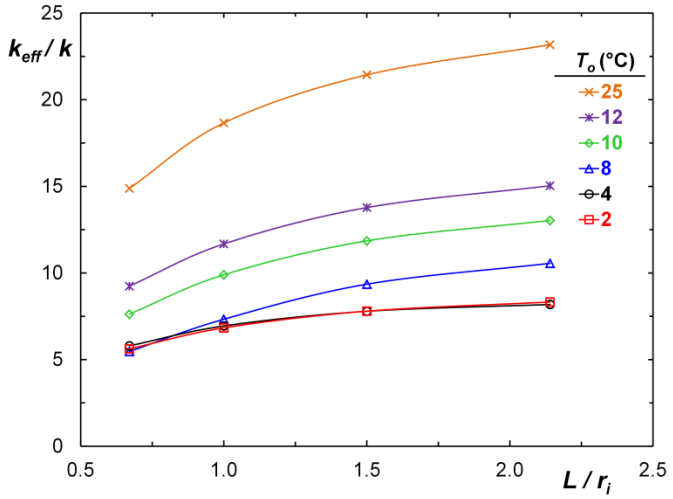

Figure 3 Effective thermal conductivity of water

On the other hand, in Figures 4 and 5, isotherms and streamline patterns are represented for two different outer surface temperatures with three spacing ratios. As seen in Figure 4(a), for T_o = 8°C and L/r_i = 0.67, two circulations cells exist in the domain. The inner zone is effective from ϕ = 0° to -90°. Hot water with higher density drops downwards and cold water near the inner sphere surface tends to upwards. Consequently, a clock-wise circulation takes place for this region. Remaining domain is dominated by a counter-clock-wise circulation zone. Increasing the spacing ratio, Fig. 4(b) and (c), induces thermal stratification for the upper side of the domain (0° < ϕ < 90°), and the outer circulation shifts through the bottom of the annulus. As a result, the inner circulation cell stuck into a narrow region under the sphere and almost disappears. Similarly, increasing the outer temperature also increases the intensity of the natural convection, and as seen in Fig. 5(a), even for the smallest spacing, the secondary circulation is effective only a small region around ϕ = -90°. Moreover, for the higher the spacing ratios, Fig. 5(b) and (c), it is clear that a jet-flow forms at the bottom of the inner sphere and hits on the outer surface at ϕ = -90°.

Table 3 Effective thermal conductivity ($0.67 \le L/r_i \le 2.14$)

$$k_{eff} = a(L/r_i)^3 + b(L/r_i)^2 + c(L/r_i) + d$$

T_o (°C)	*a*	*b*	*c*	*d*
2	0.77	-4.52	9.60	0.99
4	0.81	-4.7	9.61	1.22
8	0.0045	-1.94	8.85	0.40
10	1.18	-7.31	16.56	-0.56
12	1.27	-7.86	17.82	0.45
25	3.14	-17.05	33.28	-0.70

Comparative Study

As a last step, in order to test the validity of the equations that are suggested in Table 3, comparative results are given in Figure 6. Here, time-wise variation of the center temperature of the sphere during the melting process is given together with the numerical results. In the numerical code, two different cases are considered. In the first one, the thermal conductivity of the water is kept constant during the whole process. It is clear that, for the constant k_l case, the resultant temperature variation is far from being capture the experimental one. On the other hand, with the implementation of effective thermal conductivity of water as a function of the interface position into the numerical code, the variation of temperature remarkably approaches to the experimental measurements.

CONCLUSION

In this study, authors proposed the usage of effective thermal conductivity of water for inward process of water inside spherical container. Effective thermal conductivity values are evaluated in terms of the spacing-ratio of the annulus and the outer temperature value. The comparative results reveal that the method yields reasonable results regarding the experimental measurements and further studies may carry out to derive more accurate correlations for spherical or any other geometries that are commonly used in thermal energy storage systems.

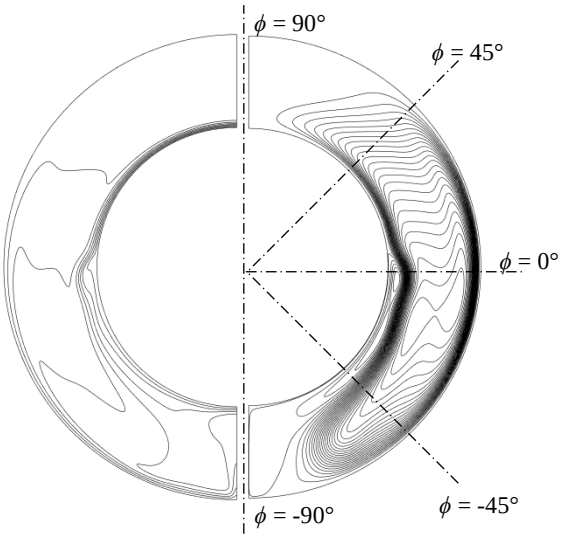

(a) L/r_i = 0.67

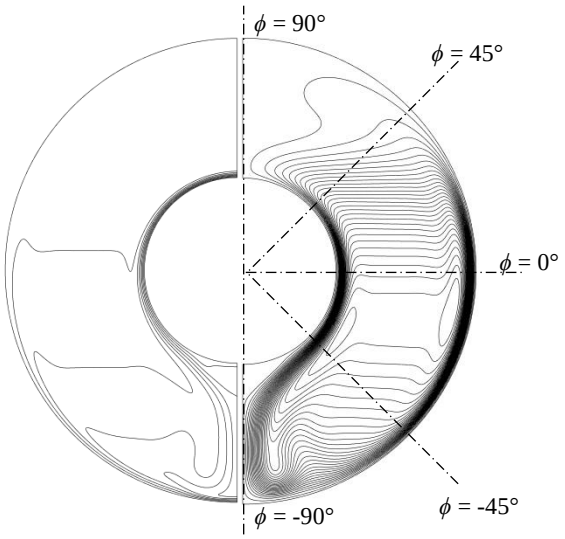

(b) L/r_i = 1.50

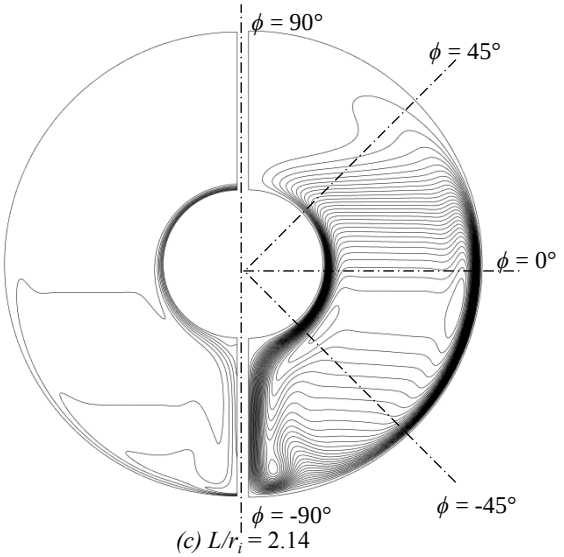

(c) L/r_i = 2.14

Figure 4 Natural convection patterns for T_o = 8°C
Isotherm(left) and streamlines (right)

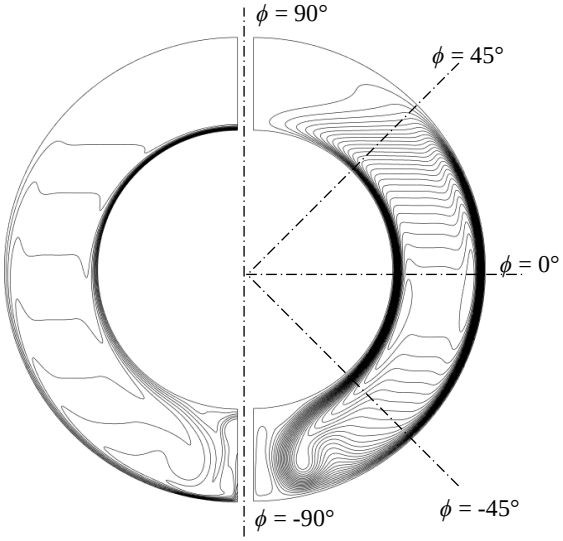

(a) L/r_i = 0.67

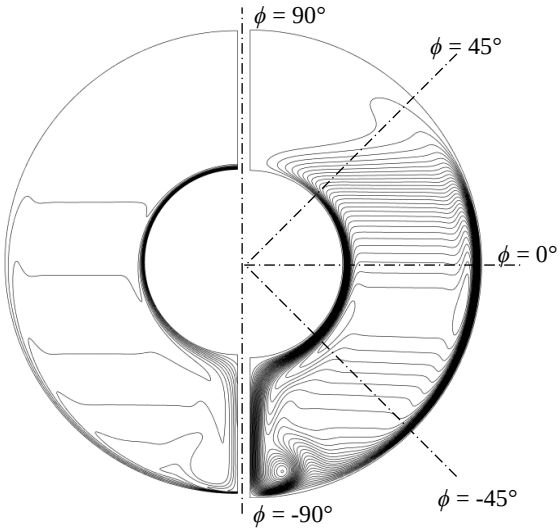

(b) L/r_i = 1.50

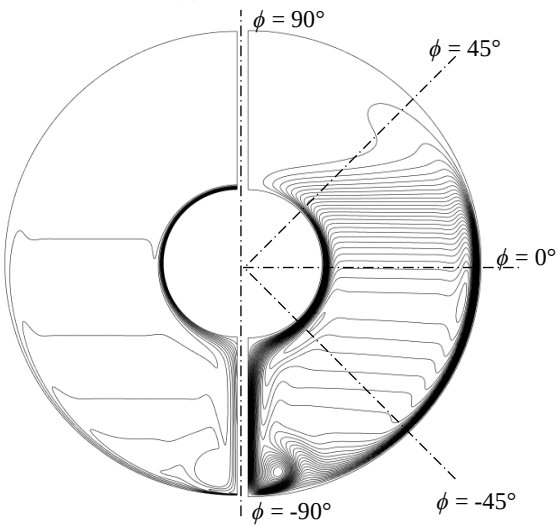

(b) L/r_i = 2.14

Figure 5 Natural convection patterns for T_o = 12°C
Isotherm(left) and streamlines (right)

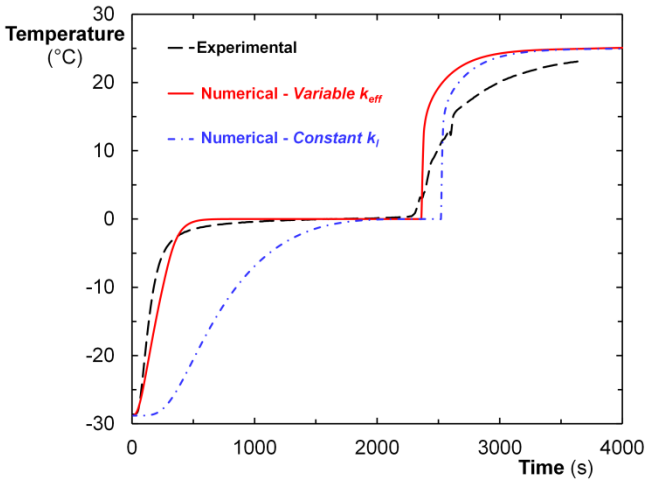

Figure 6 Comparison of experimental data with numerical findings – $T_o = 25°C$

ACKNOWLEDGEMENT

The authors would like to acknowledge the support of the Scientific and Technological Research Council of Turkey (TUBITAK) under Grant No: 112M164.

REFERENCES

[1] Huy, H., and Argyropoulos, S.A., Mathematical modelling of solidification and melting: a review, *Modelling and Simulation in Materials Science and Engineering*, Vol. 4, 1996, pp. 371–396.

[2] Voller, V.R., An overview of numerical methods for solving phase change problems, *In Advances In Numerical Heat Transfer, edited by W. J. Minkowycz, E. M. Sparrow*, Vol. 1, 1997, pp. 341-380.

[3] Dincer, I., and Rosen, M., Thermal Energy Storage: Systems and Applications, John Wiley & Sons, 2002.

[4] Tan, F.L., Hosseinizadeh, S.F., Khodadadi, J.M., and Fan, L., Experimental and computational study of constrained melting of phase change materials (PCM) inside a spherical capsule, *International Journal of Heat and Mass Transfer*, Vol. 52, 2009, pp. 3464–3472.

[5] Assis, E., Katsman, L., Ziskind, G., and Letan R., Numerical and experimental study of melting in a spherical shell, *International Journal of Heat and Mass Transfer*, Vol. 50, 2007, pp. 1790–1804.

[6] Shmueli, H., G. Ziskind, G., and Letan, R., Melting in a vertical cylindrical tube: Numerical investigation and comparison with experiments, *International Journal of Heat and Mass Transfer*, Vol. 53, 2010, pp. 4082–4091.

[7] Shatikian, V., Ziskind, G., and Letan, R., Numerical investigation of a PCM-based heat sink with internal fins, *International Journal of Heat and Mass Transfer*, Vol. 48, 2005, pp. 3689–3706.

[8] Ismail, K.A.R., Henríquez, J.R., and da Silva, T.M., A parametric study on ice formation inside a spherical capsule, *International Journal of Thermal Sciences*, Vol. 42, 2003, 881–887.

[9] Bishop E.H., Mack, L.R., and Scanlan, J.A., Heat Transfer by Natural Convection between Concentric Spheres, experiments, *International Journal of Heat and Mass Transfer*, Vol. 9. 1966, pp. 649-662.

[10] Patankar, S., Numerical heat transfer and fluid flow, Taylor & Francis, 1980.

[11] ANSYS-FLUENT 14, User's Guide, Ansys Inc., Lebanon, NH, 2003.

[12] Cao, Y., and Faghri, A., A Numerical Analysis of Phase Change Problem including Natural Convection, *ASME Journal of Heat Transfer*, Vol. 112, 1990, pp. 812-815.